

Analyzing Acoustic Radiation Modes of Baffled Plates With a Fast Multipole Boundary Element Method

Haijun Wu

e-mail: wkjiang@sjtu.edu.cn

Weikang Jiang¹

e-mail: navy_wu@sjtu.edu.cn

State Key Laboratory of Mechanical
System and Vibration
Shanghai Jiao Tong University,
Shanghai 200240, China

Yijun Liu

Mechanical Engineering,
University of Cincinnati,
Cincinnati, OH 45221-0072
e-mail: Yijun.Liu@uc.edu

In the analysis of an acoustic radiation mode of a baffled plate, Rayleigh integral with free space Green's function is involved. The boundary element method (BEM) is one of the approaches to compute its modes and radiation efficiencies. In this paper a fast multipole BEM in conjunction with an iterative solver based on the implicit restart Arnold method is proposed to efficiently and accurately evaluate acoustic radiation modes and efficiencies. Even though a 3D free space Green's function is used here, a quad tree is used for the hierarchical tree structure of the boundary mesh instead of an oct tree, which can speed up the fast multipole BEM. Similar to the analytical integration of moment evaluations, the analytical integration is also employed to compute the local expansion coefficients which further improves the efficiency of the fast multipole BEM for the analysis of an acoustic radiation mode of baffled plates. Comparison between numerical and theoretical radiation efficiencies of a baffled circular plate vibrating as a piston shows that the fast multipole BEM proposed here can give results with very good accuracy. The computation of the eigenvalues and eigenvectors of a baffled rectangular plate further reveals the efficiency in CPU time, smaller memory size, and accuracy of the fast multipole BEM in the analysis of an acoustic radiation mode. [DOI: 10.1115/1.4007023]

Keywords: acoustic radiation modes, fast multipole boundary element method, baffled plates

1 Introduction

Radiation power is the quantity widely used in active noise control, sources reconstruction, and acoustic design optimization. The radiation power of a baffled vibrating structure can be calculated by the Rayleigh integral [1] which consists of two steps, one is to determine the acoustic pressure first by boundary element method (BEM), and the other is to sum the acoustic pressure and normal velocity product over a close boundary. It is time consuming in the engineering application. An acoustic radiation mode was first proposed by the motivation of representing any boundary normal velocity using linear superposition of a set of orthonormal velocity patterns on the boundary, and then to evaluate the radiation power by using velocity patterns.

Cunefare [2] presented a technique for deriving the optimal surface velocity distribution on the surface of a finite baffled beam, in which the surface velocity was expanded in the unknown modal amplitude coefficients. Later, Cunefare and Currey [3] explored the convergence, upper bound on radiation efficiencies, and the sensitivity of the acoustic modes' radiation efficiencies to small perturbations. The term "radiation modes" was introduced first by Cunefare in his Ph.D. dissertation [4]. Elliott and Johnson compared two formulations, one was based on structure modes and the other was in terms of acoustic modes, for calculating the total acoustic power radiated by a structure in Ref. [5]. Chen and Ginsberg [6] developed a method to analyze submerged bodies' acoustic interaction using radiation modes. Snyder and Tanaka [7] calculated the total acoustic power output of a baffled rectangular using the modal radiation efficiencies.

Fahline and Koopmann [8] proposed a lumped parameter model for the acoustic output from a vibrating structure. It was based on the Kirchoff-Helmholtz equation with Neumann boundary conditions and assumed that each of the boundary elements vibrates as a piston. Actually, the underlying theory is similar to methods using the BEM with a constant element. In the evaluation of entries of the impedance matrix, Taylor series were employed to the kernel about the geometrical centers of each element and truncating all but the lowest-order (monopole) terms. In the second of their series papers [9], the lumped parameter model was implemented numerically by requiring the boundary condition for the normal surface velocity to be satisfied in a lumped parameter sense. Arenas [10] applied the lumped parameter model to compute the sound radiation from planar structures which was based on the surface velocity information and a direct numerical evaluation of the radiation resistance matrix of the structure.

As remarked in Refs. [9,10], one disadvantage of the method was the amount of computational time spent in solving the system of equations for the source amplitudes. This is a general restraint in methods involving the BEM. Thanks to the development of the fast multipole method (FMM) pioneered by Rokhlin [11] and Greengard [12], FMM can dramatically reduce the matrix vector product from $O(N^2)$ to $O(N \log N)$, and memory from $O(N^2)$ to $O(N)$ with N being the number of boundary elements in the model surface discretization. Fast multipole BEM, one of the FMM applications in the BEM, has been proved very efficient in acoustic wave problem solutions recently [13–26]. An elaborate review of the fast multipole accelerated BEM up to 2002 was made by Nishimura in Ref. [27]. More information about the fast multipole BEM in general can be found in the first textbook [28].

Similar to the fast multipole boundary element method (FMBEM) developed for acoustic wave problems, the FMM is now being extended to an acoustic radiation mode analysis as well as a sound power radiation computation. Consequently, a fast

¹Corresponding author.

Contributed by the Noise Control and Acoustics Division of ASME for publication in the JOURNAL OF VIBRATION AND ACOUSTICS. Manuscript received August 9, 2011; final manuscript received May 24, 2012; published online February 4, 2013. Assoc. Editor: Lonny Thompson.

multipole BEM is developed for an acoustic radiation mode analysis of baffled plates, which is implemented in conjunction with one iterative eigenvalue solver, the implicit restart Arnold method (IRAM) [29].

The rest of the paper is organized as follows: Acoustic radiation mode theory of baffled plates is reviewed in Sec. 2. The formulations of the fast multipole BEM for the analysis of an acoustic radiation mode are described in Sec. 3. Then, the fast multipole BEM algorithm and some remarks concerning the program implementation are made in Sec. 4. Several numerical examples are performed in Sec. 5 to demonstrate the accuracy and efficiency of the proposed fast multipole BEM in the analysis of acoustic radiation modes of baffled plates. Section 6 gives a conclusion of this paper.

2 Acoustic Radiation Mode Theory

To represent the sound power radiation of a vibrating structure by a set of independent velocity patterns on the surface of the structure, a radiation operator which relates velocity on the boundary to the sound power needs to be built. We review here the basic theory used to generate the radiation operator. Consider a structure with a boundary S excited harmonically in a homogeneous isotropic acoustic medium. A normal velocity v and sound pressure φ on the boundary S are produced by the harmonic force applied on the structure. The sound power radiated by the structure can be evaluated by taking the real part of the integral of the sound intensity over the boundary of the structure

$$W = \frac{1}{2} \text{Re} \int_S \varphi(\mathbf{x}) v(\mathbf{x})^* dS(\mathbf{x}) \quad (1)$$

where the asterisk indicates the complex conjugate for scalar variables and complex conjugate transpose for vectors and matrices, and \mathbf{x} is a point on the boundary.

The Rayleigh integral is an approximate method to represent the boundary sound pressure in terms of boundary velocity for a group of vibrating structures which can be assumed flat or near flat and baffled by an infinite plate. Sound pressure at a boundary point \mathbf{x} is expressed as

$$\varphi(\mathbf{x}) = -\frac{1}{\gamma(\mathbf{x})} k\rho c \int_S iG(\mathbf{x}, \mathbf{y}) v(\mathbf{y}) dS(\mathbf{y}) \quad (2)$$

in which $\gamma(\mathbf{x})$ is a constant that depends on the geometry of the structure at point \mathbf{x} , $\gamma(\mathbf{x}) = 1/2$ if the surface around point \mathbf{x} is smooth. The free space Green's function $G(\mathbf{x}, \mathbf{y})$ for 3D problems is given by

$$G(\mathbf{x}, \mathbf{y}) = \frac{e^{ik|\mathbf{x}-\mathbf{y}|}}{4\pi|\mathbf{x}-\mathbf{y}|} \quad (3)$$

where k is the wave number and ρ and c stand for the mass density and speed of sound of the acoustic fluid medium, respectively. Note that in this paper the time convention is assumed as $e^{-i\omega t}$ and $v(\mathbf{y})$ in Eq. (2) is the normal velocity at point \mathbf{y} on the boundary.

2.1 Rayleigh Radiation Operator. The Rayleigh integral expresses the transformation from the structure surface velocity to the boundary sound pressure, which can be used directly to build a radiation operator. Since we aim to obtain the sound power by a set of independent velocity patterns on the surface, replacing $\varphi(\mathbf{x})$ in Eq. (1) by Eq. (2) produces

$$W = -\frac{k\rho c}{2} \text{Re} \left\{ \int_S \int_S \frac{1}{\gamma(\mathbf{x})} v(\mathbf{y}) iG(\mathbf{x}, \mathbf{y}) v(\mathbf{x})^* dS(\mathbf{y}) dS(\mathbf{x}) \right\} \quad (4)$$

Use the identity $\text{Re}\{a\} = \{a + a^*\}/2$, trade \mathbf{x} for \mathbf{y} in the second integral, and further simplify Eq. (4) by using the reciprocity of the Green function and the relationship $i(G - G^*) = -2G^I$, where G^I is the imaginary part of the Green's function. Consequently, Eq. (4) can be reformulated as

$$W = \frac{k\rho c}{2} \int_S \int_S \frac{1}{\gamma(\mathbf{x})} v(\mathbf{x})^* G^I(\mathbf{x}, \mathbf{y}) v(\mathbf{y}) dS(\mathbf{y}) dS(\mathbf{x}) \quad (5)$$

To evaluate Eq. (5) we consider the normal velocity being a vector \mathbf{v} which belongs to a linear vector on the boundary S . The length of vector \mathbf{v} represents the number of elements of the discretized acoustic modes. How many discretized elements used to mesh the surface and which type of element chosen to represent the velocity distribution on an element are crucial to the convergence of the eigenstate analysis of the radiation operator and the accuracy of the evaluation of sound power radiation. Theoretically, the more elements used in the discretization, the more accurate the solution will be. Drawbacks are the high cost in the CPU time and memory requirement of using a large number of elements. CPU time and memory requirement essentially restrict the discrete representation of the radiation operator based on the conventional BEM (CBEM), especially for large-scale structure problems. But these drawbacks associated with CBEM are removed now by using the fast multipole BEM which will be described in Sec. 3.

A constant triangular element is adopted in this paper, which assumes that the sound pressure and structure velocity are constants on an element. The primary benefit of using the constant element is the convenience in implementation of the fast multipole BEM algorithm. Furthermore, the shortcoming in the accuracy of adopting the constant element can be easily eliminated by using more elements in the boundary mesh due to the high solution efficiency of the fast multipole BEM. Supposing that N is the number of elements in the boundary discretization, corresponding $\gamma(\mathbf{x}) = 1/2$, we have

$$W = \mathbf{v}^* \mathbf{R} \mathbf{v} \quad (6)$$

in which \mathbf{R} is named the radiation operator based on the Rayleigh integral, whose entries are defined as

$$r_{ij} = k\rho c \int_{\Delta S_i} \int_{\Delta S_j} G^I(\mathbf{x}, \mathbf{y}) dS(\mathbf{y}) dS(\mathbf{x}), \quad \text{for } i, j = 1, 2, \dots, N \quad (7)$$

in which ΔS_i and ΔS_j indicate the elements i and j , respectively. It is easy to conclude from Eq. (7) that \mathbf{R} is a real and symmetrical matrix by using reciprocity principle of the Green function. The sound power radiation of a vibrating plane should be positive. Any nonzero vector \mathbf{v} in Eq. (6) must result in a positive value. Therefore, \mathbf{R} is a positive definite matrix.

Note that in some literatures, such as Ref. [5], the mean value theorem of integral is employed in the evaluation of Eq. (7) by treating G^I as a slowly varying function on element pairs (i, j) . Therefore, $r_{ij} = k\rho c G^I(\mathbf{x}_i, \mathbf{y}_j) \Delta S_i \Delta S_j$ with $\mathbf{x}_i, \mathbf{y}_j$ being the centers of elements i and j , respectively, and $\Delta S_i, \Delta S_j$ being areas of the two elements. In the fast multipole BEM, faraway enough element pairs (i, j) are computed efficiently by using the FMM, and only a few of close element pairs (i, j) needed to be evaluated directly, we adopt the Gauss quadrature method to compute Eq. (7) for close element pairs (i, j) , and the FMM to evaluate Eq. (7) for faraway enough element pairs (i, j) .

2.2 Modal Analysis of Radiation Operator. The Rayleigh radiation operator is real, symmetrical, and nonsingular, which can be used to diagonalize the calculation of sound power radiation. The eigenvalues and corresponding eigenvectors of the operator \mathbf{R} are denoted by λ_i and \mathbf{u}_i , which satisfy

$$\mathbf{R}\mathbf{u}_i = \lambda_i \mathbf{u}_i, \quad \text{for } i = 1, 2, \dots, N \quad (8)$$

Based on the theorem of a positive definite matrix, operator \mathbf{R} must have N positive eigenvalues λ_i , which can be ordered as $\lambda_1 > \lambda_2 > \dots > \lambda_N > 0$. The corresponding normalized eigenvectors \mathbf{u}_i represent the velocity patterns, termed as acoustic radiation modes, which span the velocity distribution on the structure surface. Therefore, arbitrary velocity distribution \mathbf{v} on the boundary can be expanded in terms of the acoustic radiation modes as

$$\mathbf{v} = \mathbf{u}\beta \quad (9)$$

where \mathbf{U} is a unitary matrix formed by eigenvectors and β represents a vector of modal participation coefficients with entries defined as $\beta_i = \mathbf{v}^* \mathbf{u}_i$. Substituting Eqs. (9) and (8) into Eq. (6) leads directly to a simple and compact expression of the sound power radiation

$$W = \sum_{i=1}^N \lambda_i |\beta_i|^2 \quad (10)$$

In the computation of radiation power by Eq. (10), the boundary velocity patterns are divided into effective and ineffective components, which correspond to eigenvalues with large and small magnitudes, respectively. Therefore, to compute the sound power radiation by the modal expansion method, the eigenvalues with largest magnitude and corresponding eigenvectors are preferred. Since the number of eigenvalues needed to compute radiation power within a given tolerance is rarely small by comparing with the number of degrees of freedom (total number of boundary elements) of the discrete linear system, only a few eigenvalues with largest magnitude and corresponding eigenvectors are requested in the eigenvalue/eigenvector computation of the operator \mathbf{R} . As a rule of thumb, computation of the largest six in low frequency and a few more in higher frequency is necessary. The i th eigenvalue is also referred to as a variable which is proportional to radiation efficiency of the i th velocity pattern, which is defined by

$$\sigma_i = \frac{2\lambda_i}{\rho c} \quad (11)$$

Radiation efficiency (or eigenvalue) and velocity pattern (or eigenvector) are two characteristics of the radiation operator, which will be investigated in this paper by using the fast multipole BEM.

3 Fast Multipole Boundary Element Method

As shown in Eq. (7), entries of matrix \mathbf{R} are regular without involving any singular integration which can be easily and accurately integrated by using the Gaussian quadrature twice. Since the integration is required for every pair of elements, the disadvantage of expensive computational time will appear especially for large-scale models. This cost can be reduced somewhat by exploiting the symmetry of the radiation operator, but it will still require a large amount of computational time. In addition to time cost, memory requirement for storing the matrix \mathbf{R} is another defect that prevents the direct numerical method in the computation of acoustic radiation efficiencies and modes.

FMM is one of the algorithms which can accelerate the matrix vector multiplication as well as reduce the memory requirement dramatically. Employing the fast multipole BEM in the iterative solution of eigenvalues and eigenvectors, matrix \mathbf{R} is not computed explicitly but the product of \mathbf{R} and trial velocity is supplied to an iterative solver, such as IRAM. In this section we will describe the computation of contributions from all faraway enough elements to a field element i by the fast multipole BEM. Keep in mind that the contribution from an element can be added

to a field element i by the fast multipole BEM only if the element is faraway enough from the field element in the sense of tree structure. In light of Eq. (6) and using the fast multipole expansion of the kernel based on a plane wave expansion [30], contribution from all faraway enough elements to the field element i is described by

$$\begin{aligned} \phi_i = k\rho c \operatorname{Im} \left\{ \frac{ik}{16\pi^2} \int_{\sigma_1} \left[\int_{\Delta S_i} I(\hat{\boldsymbol{\sigma}}, \mathbf{x}, \mathbf{x}_c) dS(\mathbf{x}) T(\hat{\boldsymbol{\sigma}}, \mathbf{x}_c, \mathbf{y}_c) \right. \right. \\ \left. \left. \times \int_{\Delta S_j \in F_i} O(\hat{\boldsymbol{\sigma}}, \mathbf{y}_c, \mathbf{y}) v(\mathbf{y}) dS(\mathbf{y}) \right] d\sigma \right\} \quad (12) \end{aligned}$$

for $|\mathbf{x} - \mathbf{x}_c| < |\mathbf{y} - \mathbf{x}_c|$ and $|\mathbf{y} - \mathbf{y}_c| < |\mathbf{x} - \mathbf{y}_c|$, where \mathbf{x}_c is an expansion point near \mathbf{x} and \mathbf{y}_c is that near \mathbf{y} , Im means imaginary part of a complex variable, F_i is a set of all elements far away from the element i in the sense of tree hierarchical structure. The inner, translation, and outer functions in Eq. (12) are defined by

$$I(\hat{\boldsymbol{\sigma}}, \mathbf{x}, \mathbf{x}_c) = e^{ik(\mathbf{x} - \mathbf{x}_c) \cdot \hat{\boldsymbol{\sigma}}} \quad (13)$$

$$T(\hat{\boldsymbol{\sigma}}, \mathbf{x}_c, \mathbf{y}_c) = \sum_{l=0}^{\infty} i^l (2l+1) h_l^{(1)}(kt) P_l(\hat{\mathbf{t}} \cdot \hat{\boldsymbol{\sigma}}) \quad (14)$$

$$O(\hat{\boldsymbol{\sigma}}, \mathbf{y}_c, \mathbf{y}) = e^{ik(\mathbf{y}_c - \mathbf{y}) \cdot \hat{\boldsymbol{\sigma}}} \quad (15)$$

respectively, where $t = |\mathbf{x}_c - \mathbf{y}_c|$ and $\hat{\mathbf{t}} = (\mathbf{x}_c - \mathbf{y}_c)/t$, P_l is l th order Legendre function, and $\hat{\boldsymbol{\sigma}} = (\sin \theta \cos \phi, \sin \theta \sin \phi, \cos \theta)$ in which θ and ϕ are polar coordinates of point $\boldsymbol{\sigma}$ on the unit sphere σ_1 . It should be noted that the series appearing in Eq. (14) is divergent. In the numerical evaluation the series should be truncated properly. Lots of studies were devoted to analyses of the truncation error and approaches of selecting the proper truncation number [31–33]. An empirical method was proposed in [34] and was validated that it can give a good truncation number selection.

Moments for a cell centered at \mathbf{y}_c , containing a set of elements Ω , are defined by

$$M(\hat{\boldsymbol{\sigma}}, \mathbf{y}_c) = \sum_{j \in \Omega} \int_{\Delta S_j} e^{ik(\mathbf{y}_c - \mathbf{y}) \cdot \hat{\boldsymbol{\sigma}}} dS(\mathbf{y}) \quad (16)$$

The moments of all cells are computed by the upward pass which traces the tree from bottom to top. After obtaining the moments of cells, the local expansions for one cell centered at \mathbf{x}_c are evaluated by collecting the moments of its well-separated cells and transferring the local expansions from its parent cell. These well-separated cells of one cell are noted as the interaction list ℓ , the moment of all cells in a cell's interaction list are converted to the local expansions of the cell through

$$L(\hat{\boldsymbol{\sigma}}, \mathbf{x}_c) = \sum_{\mathbf{y}_c \in \ell} T(\hat{\boldsymbol{\sigma}}, \mathbf{x}_c, \mathbf{y}_c) M(\hat{\boldsymbol{\sigma}}, \mathbf{y}_c) \quad (17)$$

for $|\mathbf{x} - \mathbf{x}_c| < |\mathbf{y} - \mathbf{x}_c|$ and $|\mathbf{y} - \mathbf{y}_c| < |\mathbf{x} - \mathbf{y}_c|$, in which \mathbf{x} is a field point located in the local cell whose center is \mathbf{x}_c , \mathbf{y} is the source point located in one of the cells in the interaction list whose center is \mathbf{y}_c . Because the sample points on the unit sphere are varying from level to level, the upward and downward passes in the multilevel FMM are separated into two parts. First, in the upward pass the moments are temporarily shifted from the child level to the parent level. Conversely, in the downward pass the local expansions are temporarily shifted from the parent level to the child level. They are computed, respectively, by

$$\tilde{M}(\hat{\boldsymbol{\sigma}}, \mathbf{y}_c) = e^{ik(\mathbf{y}_c - \mathbf{y}_c) \cdot \hat{\boldsymbol{\sigma}}} M(\hat{\boldsymbol{\sigma}}, \mathbf{y}_c), \quad \text{for } |\mathbf{y} - \mathbf{y}_c| < |\mathbf{x} - \mathbf{y}_c| \quad (18)$$

$$\tilde{L}(\hat{\boldsymbol{\sigma}}, \mathbf{x}_c) = e^{ik(\mathbf{x}_c - \mathbf{x}_c) \cdot \hat{\boldsymbol{\sigma}}} L(\hat{\boldsymbol{\sigma}}, \mathbf{x}_c), \quad \text{for } |\mathbf{x} - \mathbf{x}_c| < |\mathbf{y} - \mathbf{x}_c| \quad (19)$$

in which \mathbf{y}_c and \mathbf{x}_c are centers of cells in the parent level and child level, respectively. Second, interpolations are performed over a spherical surface for temporary moments and local expansions in upward and downward passes, respectively, to reconstruct the final moments $M(\hat{\sigma}, \mathbf{y}_c)$ and local expansions $L(\hat{\sigma}, \mathbf{x}_c)$.

In the downward pass, when a leaf containing the element i is reached, the final evaluation of contributions from all faraway enough elements to the element i is computed by

$$\varphi_i = k\rho c \operatorname{Im} \left\{ \frac{ik}{16\pi^2} \int_{\sigma_1} \left[\int_{\Delta S_i} I(\hat{\sigma}, \mathbf{x}, \mathbf{x}_c) dS(\mathbf{x}) L(\hat{\sigma}, \mathbf{x}_c) \right] d\sigma \right\} \quad (20)$$

To reconstruct the contributions from all elements, the direct numerical method is still needed to aggregate the contributions from elements contained in the adjacent cell.

4 Fast Multipole BEM Algorithm

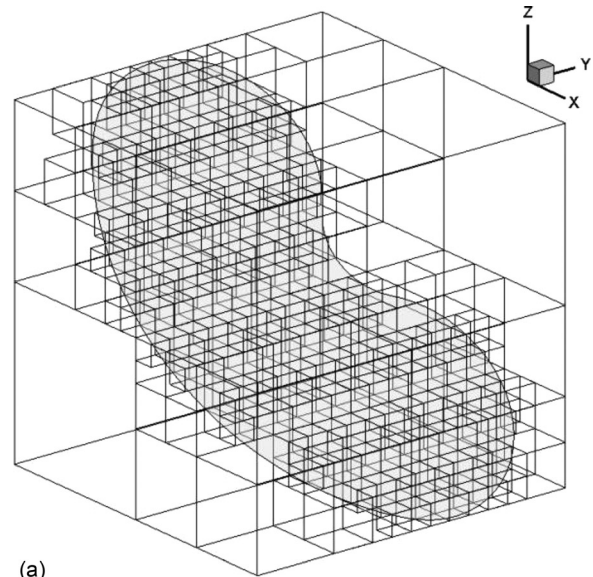
With all the formulations introduced in Sec. 3, we are ready to construct the fast multipole BEM algorithm for the analysis of an acoustic radiation mode. The FMM method used here is a variation of the algorithm presented in Ref. [26]. An iterative solver based on the implicit restart Arnold method is adopted in the eigenvalues calculation in which the product of matrix \mathbf{R} and trivial velocity \mathbf{v} is computed by the fast multipole BEM at each iteration. In this section two remarks on tree selection and analytical integration of moments and local expansion coefficients are made first. Then the main procedures of the algorithm are briefly described.

For the mode analysis of a baffled plate with the fast multipole BEM, usually an oct tree is used for the model, as shown in Fig. 1(a). Even though the kernel of the Rayleigh integral is a three-dimensional free space Green's function, we use a quad tree for the BEM model instead of an oct tree, which is permitted by rotating and moving the coordinate system to let the z axis of the new system be parallel to the normal direction of the plane, as shown in Fig. 1(b). Two benefits are achieved with this operation. First of all, it is easier to obtain the tree structure for the model by using a quad tree than an oct tree, as well as trace up and down in the moment and local expansion passes. Another benefit is related to the program optimization. M2L transformation is the most expensive part in the downward pass and at most 189 M2L translations are computed for a cell. Computing those translators once and storing them for reuse can greatly improve the efficiency of M2L. But there are 316 possible relative positions between a cell and its interaction cell at one level in an oct tree structure. That means the translators corresponding to the 316 possible relative positions need to be computed and stored. There are only 40 possible relative positions between a cell and its interaction cell in a quad tree structure, which can reduce the memory for storing the translators at one level.

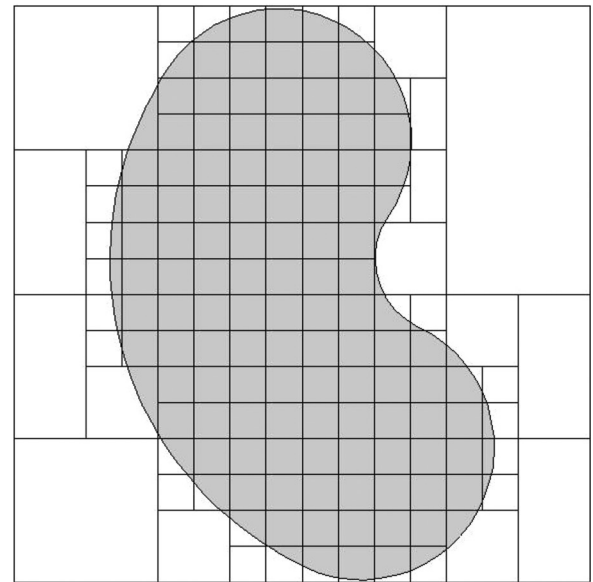
In the final evaluation Eq. (20), one more integration over a field element for sample points on the unit sphere appears. This integration does not exist in the solution of acoustic radiation and scattering problems with the usual fast multipole BEM. Since an analytical integration of moments was proposed in Ref. [26] and significant improvement in solution efficiency was achieved, the integration over a field element is no more than applying the analytical integration, same to the moments integration, one more time. It is permissible because the outer function is in essence a complex conjugate of the inner function as indicated by Eqs. (13) and (15), so that without modification the subroutine for analytical moments integration is readily used to compute the local expansion coefficients.

The main procedures of the algorithm are as follows:

Step 1. Initialization and obtain the tree structure: In this step set the number of eigenvalues and corresponding eigenvector needed to be computed first. Rotate and move the frame to let



(a)



(b)

Fig. 1 Tree structure of a plate model by using (a) an oct tree and (b) a quad tree

the z axis of the new frame be parallel to the normal direction of the plate. Then determine the quad tree structure of the mesh by dividing the model into a smaller and smaller group until the condition, either the depth of the tree or the maximum number of elements allowed in a leaf, is reached.

Step 2. Upward pass: Calculate the moments of all cells from bottom to level 2. At one level, first extrapolate the temporary moments, collecting from children cells, of a nonleaf cell to fit the sample points at this level. For a leaf cell, moments are evaluated by Eq. (16) and converted to the temporary moments by Eq. (18). Those temporary moments are added to its parent cell.

Step 3. Downward pass: Calculate the local expansions of all cells from level 2 to bottom level. At one level, first interpolate the temporary local expansion, transferring from its parent cell, of a nontop level cell to fit the sample points at this level. For a cell,

transfer moments of all cells in its interaction list and add them to its local expansions by Eq. (17). If the cell is not a leaf, its local expansions are converted temporarily to its children cells by Eq. (19). In this downward pass, if a leaf is reached, the contributions from all faraway enough elements to an element i contained in the leaf are evaluated by Eq. (20). Contributions from elements contained in the adjacent cell are computed by the direct numerical method and added to the element i .

Step 4. Iteration of the eigenvalues searching: The product of matrix \mathbf{R} and trivial velocity \mathbf{v} is supplied to an IRAM solver to compute the eigenvalues/eigenvectors. If the number of eigenvalues/eigenvectors computed or the iteration times used does not reach the specified number, update \mathbf{v} and go back to step 2. Otherwise, solution is done.

The algorithm described here is based on a normal quad tree structure. The adaptive tree algorithm presented in Refs. [23,25] can be adopted to further improve the M2L computation efficiency, in which the interaction list is divided into three groups.

5 Numerical Examples

The algorithm presented in this paper for mode analysis of the acoustic radiation operator is implemented into a compute coder. The IRAM will add an eigenvalue in the iteration eigenvalue searching if the residue is below the tolerance of 10^{-5} . All the computations were done on a desktop PC with a 64-bit Intel® Core™2 Duo CPU and 6 GB RAM, but only one core is used in the computation.

5.1 Validation of the Algorithm. Before the code can be used with confidence, accuracy of the algorithm should be verified. Because analytical formulation of the radiation efficiency is available, the radiation efficiency of a baffled circular plate is selected to explore the accuracy of the fast multipole BEM proposed in this paper. The acoustic radiation efficiency of a vibrating structure with normal boundary velocity v is defined as

$$\sigma = \frac{W}{\rho c \int_S v(\mathbf{x})^2 dS(\mathbf{x}) / 2} \quad (21)$$

Supposing the baffled circular plate is vibrating like a rigid piston with a constant velocity, and its radius is a , the radiation efficiency is defined by [35]

$$\sigma = 1 - \frac{J_1(2ka)}{ka} \quad (22)$$

Theoretical radiation efficiency is evaluated by Eq. (22), and numerical radiation efficiency is calculated according to Eq. (21) with W being computed by the fast multipole BEM. Since the fast multipole BEM adopted in this paper is a diagonal one, numerical instability will happen if ka is too small [36,37]. On the other hand, if ka is too small, very few elements are needed to discretize the boundary, which may be solved more efficiently by the conventional BEM than the fast multipole BEM. So in this study, the radiation efficiency for the baffled circular plate are evaluated at relatively high frequencies with ka from 0.5 to 30. The number of elements (DOFs) are listed in Table 1. The sole restriction in the discretization is to avoid the numerical instability for the lower ka cases. There is no doubt that the number of elements chosen in the

Table 1 Number of elements for different ka used in the FMBEM

ka	[0.5, 1]	(1, 2]	(2, 5]	(5, 10]	(10, 20]	(20, 30]
DOFs	694	904	2402	4544	8012	11272
TreLev	2	3	4	5	5	5

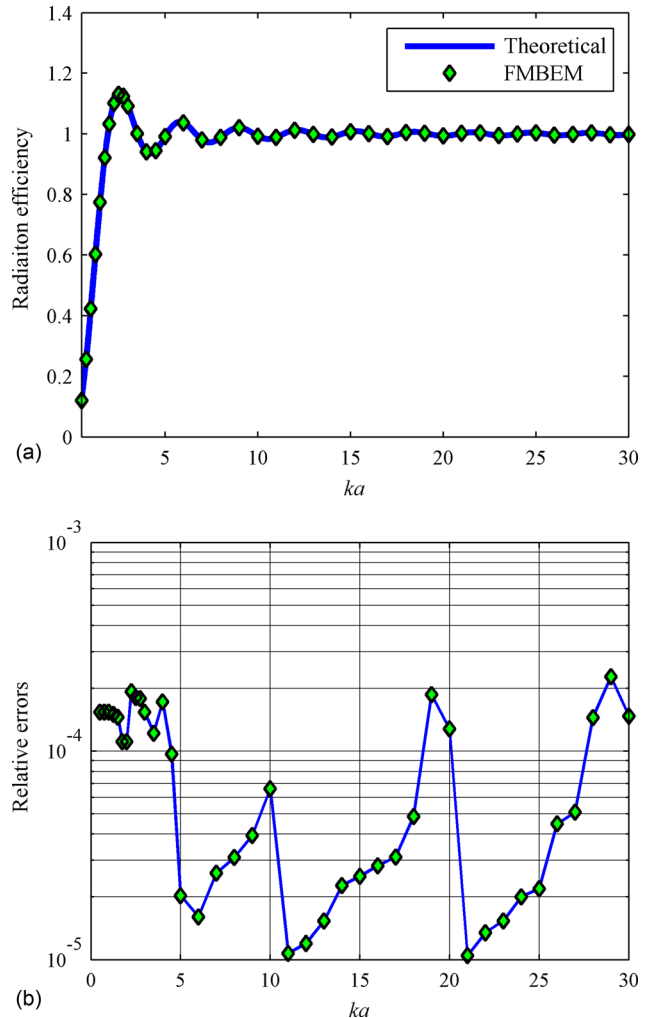


Fig. 2 (a) Radiation efficiency of a baffled circular plate calculated numerically and theoretically and (b) the relative errors

simulation is larger than the empirical rule six boundary elements per wavelength. The quad tree levels (TreLev) used in the model hierarchization are also included in Table 1.

The radiation efficiencies calculated by the fast multipole BEM and theoretical formulation are plotted in Fig. 2(a) and the relative errors defined by $|FMBEM - Theoretical| / |Theoretical|$ are plotted in Fig. 2(b). As depicted in Fig. 2, the numerical results agree very well with theoretical results. The tendency for relative errors goes up with ka increasing at a certain range as shown in Fig. 2(b). It does explain that the boundary discretization in acoustics should depend on the nondimensional wave number ka .

5.2 Modal Analysis of a Baffled Rectangular Plate. After the accuracy verification, in this section the fast multipole BEM is

Table 2 The first six eigenvalues and relative errors

Modes	Eigenvalues			Eigenvectors
	FMBEM	Direct	Relative error	Relative error
Mode 1	4.7978×10^{-2}	4.7978×10^{-2}	6.2528×10^{-9}	2.5208×10^{-7}
Mode 2	3.0495×10^{-2}	3.0495×10^{-2}	1.6396×10^{-8}	7.4120×10^{-8}
Mode 3	1.4138×10^{-2}	1.4138×10^{-2}	5.6583×10^{-8}	3.5601×10^{-7}
Mode 4	5.6936×10^{-3}	5.6936×10^{-3}	1.1943×10^{-7}	7.0494×10^{-7}
Mode 5	5.3770×10^{-3}	5.3770×10^{-3}	2.1201×10^{-7}	4.4989×10^{-7}
Mode 6	6.9162×10^{-4}	6.9162×10^{-4}	1.0700×10^{-7}	1.1662×10^{-7}

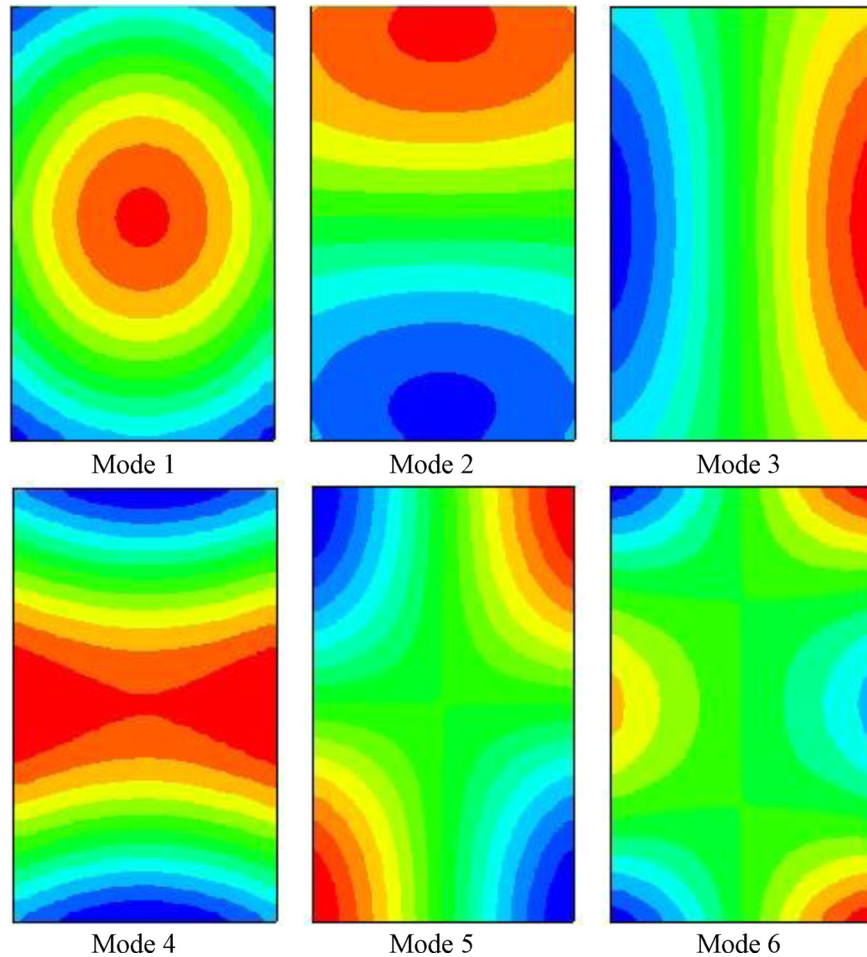


Fig. 3 The first six radiation modes of a rectangular plate

combined with the iterative solver IRAM to compute the modes and corresponding radiation efficiencies of a baffled rectangular plate. The usage of a rectangular plate to produce sound in engineering is widespread. A large body of research has been devoted to their study. Since the physical explanations of the modes and radiation efficiencies have been intensively explored, here we just focus on the CPU time, memory, and accuracy given by the fast multipole BEM. The ratio of width d to length a of the rectangular plate used here is $d/a = 0.6$.

In the first case, nondimensional wave number ka is equal to 5, the rectangular plate is meshed with 3000 triangular elements. The six eigenvalues of largest magnitude and their corresponding eigenvectors are computed by the fast multipole BEM, and by the conventional direct BEM, respectively. The six eigenvalues and the corresponding relative errors, which are calculated by $|\text{FMBEM} - \text{Direct}|/|\text{Direct}|$, are listed in Table 2. The six eigenvectors contours computed by FMBEM are plotted in Fig. 3, and their relative errors with respect to that calculated by direct BEM in L2 sense are contained in Table 2.

The efficiency of the fast multipole BEM for the analysis of an acoustics mode is investigated next. The nondimensional wave number ka is set to 15. The number of elements (DOFs) used to

Table 3 Memory used in the direct BEM and fast multipole BEM

DOFs	1044	2100	4130	6106	11,136	21,140	43,930	75,000
Direct	8.3156	33.646	130.13	284.45	946.13	3109.6*	14,723*	42,915*
(Mb)								
FMBEM	3.601	5.325	9.135	11.511	22.764	32.781	77.237	190.627
(Mb)								

discretize the model is increasing from 1000 to 75,000, as shown in Table 3. The maximum element number allowed in a leaf is set to 20. Fifteen eigenvalues of largest magnitude and their corresponding eigenvectors are requested in the computation. Eigenvalues and eigenvectors for the radiation operator of the rectangular plate are computed by the direct BEM with a solver supplied in LAPACK [38], by the direct BEM with IRAM solver, and by the fast multipole BEM with IRAM solver, respectively. Due to the

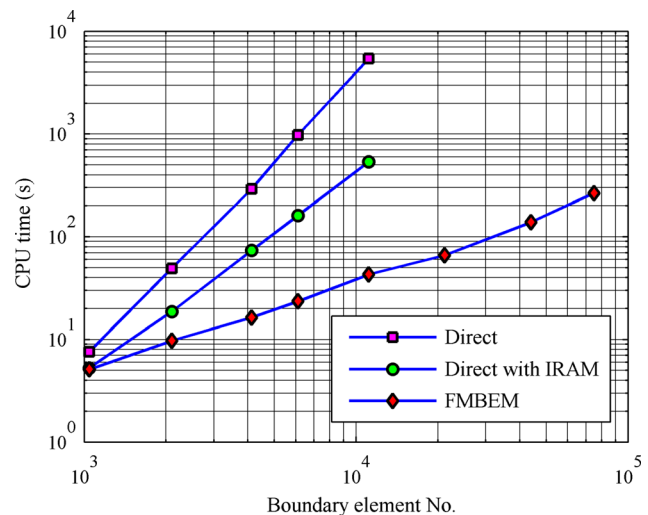


Fig. 4 CPU time of the direct BEM and fast multipole BEM

disadvantage of conventional BEM in memory, eigenvalue and eigenvector computations with the direct BEM can just be performed for DOFs up to 11,136 on our desktop PC. The CPU time taken by the three methods denoted as direct, direct with IRAM, and FMBEM are plotted in Fig. 4. Their memory usage is listed in Table 3, in which * means estimated memory. The number of iterations used by the fast multipole BEM with the IRAM solver for all cases is 31.

The above examples clearly demonstrate the accuracy, efficiency in CPU time, and advantage in memory usage of the fast multipole BEM in the analysis of an acoustics radiation mode. It gives a promising way in the analysis of an acoustic radiation mode for large-scale baffled plates.

6 Conclusion

A fast multipole BEM in conjunction with the IRAM solver is proposed for the analysis of an acoustic radiation mode of baffled plates. A baffled circular plate vibrating with constant velocity, which has an analytical radiation efficiency formula, is used first to verify the accuracy of the fast multipole BEM. Numerical results show that the fast multipole BEM can give very good results. Then, the accuracy of the fast multipole BEM in computing eigenvalues and eigenvectors is investigated by comparing with results given by the direct BEM for a baffled rectangular plate. Finally, comparisons of CPU time and memory usage are presented between the direct BEM and fast multipole BEM, which reveal the potential of the fast multipole BEM in the analysis of an acoustic radiation mode of a large-scale baffled plate.

The developed fast multipole BEM algorithm can be readily extended to the analysis of an acoustic radiation mode for three-dimensional large-scale problems, which are more general than the baffled plate method. But the radiation operator derived from the collection BEM for the three-dimensional problems is not symmetric, which is not suitable to be used in analysis of an acoustic radiation mode. A fast multipole BEM algorithm based on a variational BEM in conjunction with the IRAM solver for the analysis of an acoustic radiation mode of three-dimensional problems is under development.

Acknowledgment

The work is supported by Grant 11074170 of the National Natural Science Foundation of China and Grant MSVMS201105 of the National State Key Laboratory Foundation. The authors would also like to thank Dr. Guo-Qing Yuan for discussions on the theory of the acoustic radiation mode.

References

- [1] Kirkup, S. M., 1994, "Computational Solution of the Acoustic Field Surrounding a Baffled Panel By the Rayleigh Integral Method," *Appl. Math. Model.*, **18**(7), pp. 403–407.
- [2] Cunefare, K. A., 1991, "The Minimum Multimodal Radiation Efficiency of Baffled Finite Beams," *J. Acoust. Soc. Am.*, **90**(5), pp. 2521–2529.
- [3] Cunefare, K. A., and Currey, M. N., 1994, "On the Exterior Acoustic Radiation Modes of Structures," *J. Acoust. Soc. Am.*, **96**(4), pp. 2302–2312.
- [4] Cunefare, K. A., 1990, "The Design Sensitivity and Control of Acoustic Power Radiated By Three-Dimensional Structures," Ph.D. thesis, Pennsylvania State University, University Park, PA.
- [5] Elliott, S. J., and Johnson, M. E., 1993, "Radiation Modes and the Active Control of Sound Power," *J. Acoust. Soc. Am.*, **94**(4), pp. 2194–2204.
- [6] Chen, P. T., and Ginsberg, J. H., 1995, "Complex Power, Reciprocity, and Radiation Modes for Submerged Bodies," *J. Acoust. Soc. Am.*, **98**(6), pp. 3343–3351.
- [7] Snyder, S. D., and Tanaka, N., 1995, "Calculating Total Acoustic Power Output Using Modal Radiation Efficiencies," *J. Acoust. Soc. Am.*, **97**(3), pp. 1702–1709.
- [8] Fahline, J. B., and Koopmann, G. H., 1996, "A Lumped Parameter Model for the Acoustic Power Output From a Vibrating Structure," *J. Acoust. Soc. Am.*, **100**(6), pp. 3539–3547.

- [9] Fahline, J. B., and Koopmann, G. H., 1997, "Numerical Implementation of the Lumped Parameter Model for the Acoustic Power Output of a Vibrating Structure," *J. Acoust. Soc. Am.*, **102**(1), pp. 179–192.
- [10] Arenas, J. P., 2008, "Numerical Computation of the Sound Radiation From a Planar Baffled Vibrating Surface," *J. Comput. Acoust.*, **16**(3), pp. 321–341.
- [11] Rokhlin, V., 1985, "Rapid Solution of Integral Equations of Classical Potential Theory," *J. Comput. Phys.*, **60**(2), pp. 187–207.
- [12] Greengard, L., and Rokhlin, V., 1987, "A Fast Algorithm for Particle Simulations," *J. Comput. Phys.*, **73**(2), pp. 325–348.
- [13] Amini, S., and Profit, A. T. J., 2003, "Multi-Level Fast Multipole Solution of the Scattering Problem," *Eng. Anal. Bound. Elem.*, **27**(5), pp. 547–564.
- [14] Chen, J. T., and Chen, K. H., 2004, "Applications of the Dual Integral Formulation in Conjunction With Fast Multipole Method in Large-Scale Problems for 2D Exterior Acoustics," *Eng. Anal. Bound. Elem.*, **28**(6), pp. 685–709.
- [15] Fischer, M., Gauger, U., and Gaul, L., 2004, "A Multipole Galerkin Boundary Element Method for Acoustics," *Eng. Anal. Bound. Elem.*, **28**(2), pp. 155–162.
- [16] Gumerov, N. A., and Duraiswami, R., 2005, "Computation of Scattering From Clusters of Spheres Using the Fast Multipole Method," *J. Acoust. Soc. Am.*, **117**(41), pp. 1744–1761.
- [17] Fischer, M., and Gaul, L., 2005, "Application of the Fast Multipole BEM for Structural-Acoustic Simulations," *J. Comput. Acoust.*, **13**(1), pp. 87–98.
- [18] Gumerov, N., and Duraiswami, R., 2004, *Fast Multipole Methods for the Helmholtz Equation in Three Dimensions*, Elsevier, New York.
- [19] Gaul, L., and Fischer, M., 2006, "Large-Scale Simulations of Acoustic-Structure Interaction Using the Fast Multipole BEM," *ZAMM-Z. Angew. Math. Me.*, **86**(1), pp. 4–17.
- [20] Cheng, H., Crutchfield, W. Y., Gimbutas, Z., Greengard, L. F., Ethridge, J. F., Huang, J., Rokhlin, V., Yarvin, N., and Zhao, J., 2006, "A Wideband Fast Multipole Method for the Helmholtz Equation in Three Dimensions," *J. Comput. Phys.*, **216**(1), pp. 300–325.
- [21] Shen, L., and Liu, Y. J., 2007, "An Adaptive Fast Multipole Boundary Element Method for Three-Dimensional Acoustic Wave Problems Based on the Burton-Miller Formulation," *Comput. Mech.*, **40**(3), pp. 461–472.
- [22] Tong, M. S., Chew, W. C., and White, M. J., 2008, "Multilevel Fast Multipole Algorithm for Acoustic Wave Scattering By Truncated Ground With Trenches," *J. Acoust. Soc. Am.*, **123**(5), pp. 2513–2521.
- [23] Bapat, M. S., Shen, L., and Liu, Y. J., 2009, "Adaptive Fast Multipole Boundary Element Method for Three-Dimensional Half-Space Acoustic Wave Problems," *Eng. Anal. Bound. Elem.*, **33**(8–9), pp. 1113–1123.
- [24] Gumerov, N. A., and Duraiswami, R., 2009, "A Broadband Fast Multipole Accelerated Boundary Element Method for the Three Dimensional Helmholtz Equation," *J. Acoust. Soc. Am.*, **125**(1), pp. 191–205.
- [25] Bapat, M. S., and Liu, Y. J., 2010, "A New Adaptive Algorithm for the Fast Multipole Boundary Element Method," *CMES-Comp. Model. Eng.*, **58**(2), pp. 161–183.
- [26] Wu, H. J., Liu, Y. J., and Jiang, W. K., 2012, "Analytical Integration of the Moments in the Diagonal Form Fast Multipole Boundary Element Method for 3-D Acoustic Wave Problems," *Eng. Anal. Bound. Elem.*, **36**(2), pp. 248–254.
- [27] Nishimura, N., 2002, "Fast Multipole Accelerated Boundary Integral Equation Methods," *Appl. Mech. Rev.*, **55**(4), pp. 299–324.
- [28] Liu, Y. J., 2009, *Fast Multipole Boundary Element Method: Theory and Applications in Engineering*, Cambridge University Press, Cambridge, UK.
- [29] Sorens, D. C., 1996, "Implicitly Restarted Arnoldi/Lanczos Methods for Large Scale Eigenvalue Calculations," No. 96-40, Institute for Computer Applications in Science and Engineering, Hampton, VA.
- [30] Rahola, J., 1996, "Diagonal Forms of the Translation Operators in the Fast Multipole Algorithm for Scattering Problems," *Bit*, **36**(2), pp. 333–358.
- [31] Koc, S., Song, J., and Chew, W. C., 1999, "Error Analysis for the Numerical Evaluation of the Diagonal Forms of the Scalar Spherical Addition Theorem," *SIAM J. Numer. Anal.*, **36**(3), pp. 906–921.
- [32] Amini, S., and Profit, A., 2000, "Analysis of the Truncation Errors in the Fast Multipole Method for Scattering Problems," *J. Comput. Appl. Math.*, **115**(1–2), pp. 23–33.
- [33] Darve, E., 2001, "The Fast Multipole Method I: Error Analysis and Asymptotic Complexity," *SIAM J. Numer. Anal.*, **38**(1), pp. 98–128.
- [34] Coifman, R., Rokhlin, V., and Wandzura, S., 1993, "The Fast Multipole Method for the Wave Equation: A Pedestrian Prescription," *IEEE Antenn. Propag. M.*, **35**(3), pp. 7–12.
- [35] Kim, Y. H., 2010, *Sound Propagation: An Impedance Based Approach*, Wiley, Singapore.
- [36] Greengard, L., Huang, J., Rokhlin, V., and Wandzura, S., 1998, "Accelerating Fast Multipole Methods for the Helmholtz Equation at Low Frequencies," *IEEE Comput. Sci. Eng.*, **5**(3), pp. 32–38.
- [37] Darve, E., and Havé, P., 2004, "Efficient Fast Multipole Method for Low-Frequency Scattering," *J. Comput. Phys.*, **197**(1), pp. 341–363.
- [38] Anderson, E., Bai, Z., Bischof, C., Blackford, S., Demmel, J., Dongarra, J., Croz, J. D., Greenbaum, A., Hammarling, S., McKenney, A., and Sorensen, D., 1999, *LAPACK User's Guide*, Society for Industrial and Applied Mathematics (SIAM), Philadelphia.